Research Article | Vol. 26, No. 26 | 24 Dec 2018 | OPTICS EXPRESS 34142
Optics EXPRESS

Fast switching, high contrast and high resolution liquid crystal device for virtual reality display

JEONG HWAN YOON,[1,3] SEUNG JAE LEE,[2,3] YOUNG JIN LIM,[2] EO JIN SEO,[2] HOON SUB SHIN,[2] JAE-MIN MYOUNG,[1,4] AND SEUNG HEE LEE[2,*]

[1]*Department of Materials Science and Engineering, Yonsei University, Seoul 03722, South Korea*
[2]*Applied Materials Institute for BIN Convergence, Department of BIN Convergence Technology and Department of Polymer Nano Science and Technology, Chonbuk National University, Jeonju, Jeonbuk, 54896, South Korea*
[3]*Both authors contribute equally*
[4]*jmmyoung@yonsei.ac.kr*
[*]*lsh1@chonbuk.ac.kr*

Abstract: Virtual reality-head mounted displays require a display with high resolution over 2000 ppi, super-fast response time and high contrast ratio for realizing super image quality at near-eyes. Several liquid crystal devices utilizing fringe-field switching (FFS) mode, having response times less than of half of conventional FFS mode, were proposed for this purpose. However, its contrast ratio is still less than 2000:1 because of intrinsic electro-optic characteristics of homogenous alignment mode and also realizing high resolution like 2000 ppi has some difficulty because twist deformation of liquid crystals can easily affect liquid crystal orientation near pixels. In this paper, we propose a vertically aligned liquid crystal device in which bend deformation occurs in a confined area by an oblique electric field, exhibiting 4 times faster decay response time than that of conventional FFS mode, higher contrast ratio over 5000:1, and pixel pitch less than 4 μm. The proposed liquid crystal device has a strong potential to be the main display for high-resolution virtual reality over 2000 ppi.

1. Introduction

Virtual reality (VR)/augmented reality (AR)-head mounted displays become very important subjects recently because it has strong potential to be electronic displays for all kinds of applications [1]. Two main display devices such as thin-film transistor (TFT) - liquid crystal displays (LCDs) and organic light-emitting-diodes (OLEDs) compete each other in this field. OLEDs could display excellent moving pictures but has some difficulty in making high resolution over 1000 ppi. On the other hands, LCDs have some disadvantage in displaying moving pictures because its response time is relatively slow compared to the emissive displays and also have difficulty in achieving such as a high resolution over 2000 ppi. For high resolution LCDs, fringe-field switching (FFS) mode is widely used owing to the high aperture ratio, high transmittance, low operation voltage and touch-screen tolerance [2–6] and many studies are reported to utilize the FFS mode for VR displays. In the FFS mode, the elastic deformation of nematic liquid crystal (LC) driven by electric field is associated with twist so that its decay response time is mainly determined by elastic restoring force associated with twist elastic constant K_2 of LC so that its decay time is relatively slow compared to a vertical alignment mode in which it is associated with K_3 because K_3 is much larger than K_2.

Several liquid crystal devices utilizing either FFS or in-plane switching (IPS) mode which shows response times less than of half of conventional FFS mode by adopting non-response LC zones were proposed for this purpose, however, its contrast ratio (CR) is still less than 2000:1 because of intrinsic electro-optic characteristics of homogenous alignment mode. In

#345651 https://doi.org/10.1364/OE.26.034142
Journal © 2018 Received 12 Sep 2018; revised 18 Nov 2018; accepted 18 Nov 2018; published 17 Dec 2018

Optics EXPRESS

addition, realizing high resolution like 2000 ppi has some difficulty because twist deformation of liquid crystals can easily affect liquid crystal orientation near pixels [7–10].

In this paper, we propose a novel liquid crystal device which can realize a high resolution over 2000 ppi, fast response time of few ms and a high contrast ratio over 5000, named ultra-fine resolution switching (UFS) device.

2. Structure and switching principle of UFS device and its advantages for high-contrast, high-resolution, and fast-response LCDs

In a voltage off-state of the UFS device, liquid crystal molecules with positive dielectric anisotropy are vertically aligned between two substrates, as shown in Fig. 1(a). A bottom substrate has two electrode layers: pixel and common transparent electrode with passivation layer between them. The common electrode has an open area with some electrode gap (g). A top substrate has a plane transparent electrode but its electrical signal is connected to the bottom common one. In this way, when a bias voltage is applied to the pixel electrode, the vertical (E_z) as well as oblique (E_z and E_x) electric field is formed depending on electrode positions, that is, a pure vertical electric field is formed in the open gap but oblique electric fields are formed at both edges of the open gap with its field directions opposite to each other, as shown in Fig. 1(b).

The normalized transmitted light (T/T_0) of an incident light in which a uniaxial nematic LC medium exists under crossed polarizers is given by

$$\frac{T}{T_0} = \sin^2\left(2\psi(V)\right)\sin^2\left(\frac{\pi d\Delta n(V)}{\lambda}\right), \tag{1}$$

where ψ is a voltage-dependent angle between the transmission axes of the crossed polarizers and the projection of the LC director onto the xy-plane, d is the cell gap, Δn is the voltage-dependent birefringence of LC, and λ is the wavelength of an incident light. The device appears to be a dark state in a voltage-off state and speaking with emphasis, its dark state is much more perfect than that of the FFS device because ψ is perfectly zero in the UFS device while ψ cannot be perfectly zero because of existence of a fabrication process error in the FFS device (this is why vertical alignment mode gives rise to CR higher than 5000: 1 while it is less than 2000:1 in a homogenous alignment mode). As indicated in Fig. 1(b), the oblique electric fields deform vertically aligned LC to be bent in both left and right directions having $\psi = 45°$, forming two-domain like LC configuration, and then the transmittance appears.

In all nematic LC devices, a rise response time (τ_r) is strongly dependent on applied voltages and thus it can be faster by applying a higher voltage. However, a decay response time (τ_d) is associated with elastic restoring force of LC cell, such that it mainly depends on d and visco-elastic property of LC, that is, $\tau_d = \gamma d^2/\pi^2 K$ where γ is the rotational viscosity and K is the elastic constant of LCs. For a FFS mode or in-plane switching (IPS) mode, K is replaced by twist elastic constant K_2 of which its amplitude is about two-thirds of splay (K_1) and one-third of bend (K_3) elastic constant. Consequently, τ_d is relatively slow compared to that of a vertical alignment mode associated with K_3 assuming that γ and d are the same each other for both modes. In order to overcome such an intrinsic issue of both FFS/IPS modes, Matsushima etal., proposed short-range lurch control (SLC)-IPS mode in which the lateral distance l between the two non-responsive LC region exists under the applied field [7,11]. In such a condition, τ_d is modified into

$$\tau_d = \frac{\gamma}{\pi^2\left(\frac{K_2}{d^2}+\frac{K_1}{l^2}\right)}, \tag{2}$$

Optics EXPRESS

and when $K_1 = 2K_2$ and $l = d$, $\tau_{d\text{-}SLC} = (\gamma d^2/3\pi^2 K_2) = \tau_{d\text{-}IPS}/3$, that is, the τ_d of SLC-IPS mode becomes three times faster than that of the conventional IPS mode. In the UFS mode, the distance l between imaginary walls in which LC does not reorient by the field exists as defined in Fig. 1(b) and an elastic deformation of LC director is associated with K_3 so that K_1 is replaced by K_3 in Eq. (2). Therefore, when $K_3 = 3K_2$ and if $l = d/2$, $\tau_{d\text{-}UFS} = (\gamma d^2/13\pi^2 K_2) \fallingdotseq \tau_{d\text{-}IPS}/13$, that is, the decay response time of the UFS-mode can be about thirteen times faster than that of the conventional IPS mode.

A short explanation why the device is advantageous to realize ultra-high resolution follows. In about 3" TFT-LCDs with 2000 ppi resolution, the pixel size is 4 μm x 12 μm in which signal lines, transistor and pixel electrode should be positioned within 4 μm data. Therefore, the smaller the pixel size, more space is allowed to the data line. In the device, the pixel size can be about the same as the g, which can be varied from 1 to 3 μm depending on an optimal design and in addition, noise fields from the data lines can be easily screened by the common electrode above pixel. In addition, forming a storage capacitor (C_{st}) is required in TFT-LCDs which may cause the loss of transmittance. However, for UFS device it is automatically formed between pixel and common electrode without sacrificing an aperture ratio (see Fig. 2(a)), which allows the device to realize high resolution without an optical crosstalk [12,13]. In fact, in-plane field driven vertical alignment device using a positive dielectric anisotropic LC [14,15] and three electrodes vertical alignment display with a negative dielectric anisotropic LC [16] was reported already; however those approaches can be very difficult to realize over 1000 ppi practical TFT-LCDs and their switching behavior and LC orientation is different from that of UFS device.

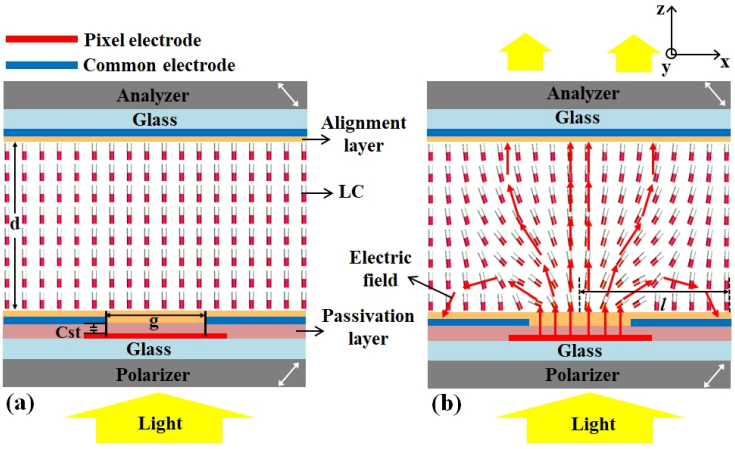

Fig. 1. Schematic cross-sectional view of the UFS device with LC director and electric field lines in (a) dark and (b) bright state. The red arrows indicate electric field direction between pixel and common electrodes. Even in voltage-on state, the distance l in which LC does not reorient by the field exists as indicated in Fig. 1(b).

3. Results and discussion

To test a feasibility of the UFS device, a numerical simulation was done by a well-known commercialized multi-dimensional finite element method (FEM) solver (TechWiz LCD, Sanayi system). The distribution of electric potential was calculated by Laplace's equation, and the optical transmittance was generated based on the [2 × 2] extended Jones matrix method. To understand field-response of LC directors, common electrode structures with three different open gaps (gs) of 1 μm, 2 μm, and 3 μm on a bottom substrate were evaluated and the thickness of passivation layer between pixel and common electrodes was 300 nm. The physical properties of LCs tested are as follows: dielectric anisotropy $\Delta\varepsilon = 8.2$, birefringence

Optics EXPRESS

Δn = 0.1148 at 550 nm, rotational viscosity γ = 80 mPa·s, splay/twist/bend elastic constants = 16.9/8.42/19.2 in pN and the d is 4 μm.

Figure 2 shows calculated electro-optic characteristics of UFS devices. The transmittance above a center of opened gap does not occur because the pure E_z keeps an original orientation of LC director and also the width of no transmittance region increases slightly with increasing size of g given a pixel pitch of 8 μm (see Fig. 2(a), 2(b) and 2(c)). However, increasing g intensifies E_x in oblique field at both sides of the open gap so that more LC molecules tilt down, that is, more phase retardation is induced as g becomes larger, resulting in a higher transmittance. Voltage-dependent transmittance indicated that maximal transmittance decreases and threshold voltage (V_{th}) increases as g becomes smaller, as shown in Fig. 2(d).The two-dimensional inset images at 0 V and 10 V when g = 2 μm in Fig. 2(d) shows transmittance profile in a black and a bright state, respectively. At 10 V, the transmittance also occurs near edges of the open gap in vertical direction. In the UFS device, the smaller g the intensity of oblique electric field becomes weaker so that the transmittance becomes lower. Response times between UFS and FFS devices by applying 10 V and 6.2 V, respectively, are compared, as shown in Fig. 2(e). Since both modes use the same LC and cell gap, its response behavior is purely determined by intrinsic device characteristics. Rise response times (τ_rs) of FFS and UFS (g = 2 μm) devices are 13.2 ms and 8.5 ms, respectively, such that about 34% becomes shorter in the UFS device. Further, 8.5 ms could be reduced to less than 3.4 ms by overdriving scheme [17]. Very impressively, the τ_d of the UFS device becomes ultra-fast such that 21.1 ms in the FFS device is reduced to 1.6 ms in the UFS device, that is, about 13 times becomes faster. In this case, $K_3 = 2.28K_2$ and l is 2.9 μm (l/d = 0.725), so that $\tau_{d\text{-UFS}} \fallingdotseq \tau_{d\text{-IPS}}$ /5.3, which does not explain fully 13 times reduction of τ_d in the UFS device though it is clear that the super-fast response of the UFS device originates from both high bend elastic constant and short distance of nonresponsive LC region. In order to explain such the reduction in τ_d, l needs to be redefined with adoption of effective distance since the bend deformation of a vertically aligned is very little for a low transmittance. If we redefine l_{eff} from a distance to a distance with transmittance of 15% (average tilt angle is about 73.7°) with respect to the maximal transmittance as defined in Fig. 2(b), then l_{eff} becomes 1.7 μm (l/d = 0.425), so that $\tau_{d\text{-UFS}} \fallingdotseq \tau_{d\text{-IPS}}$ /13.6, which explains the reduction more reasonably.

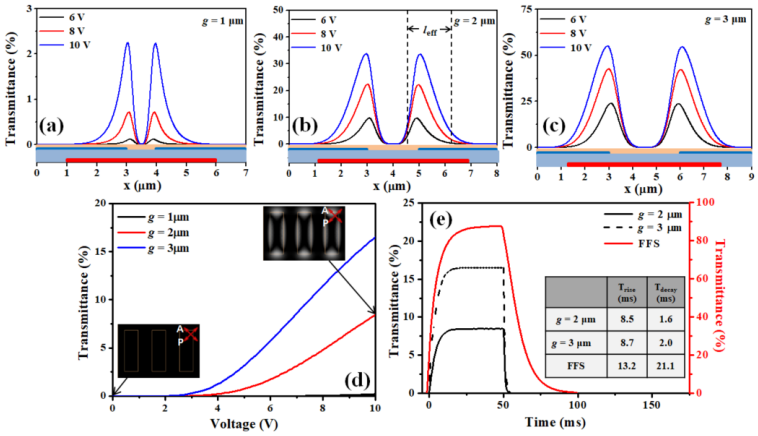

Fig. 2. Calculated electrode-position dependent transmittances at three different voltages when g is (a) 1 μm, (b) 2 μm, and (c) 3 μm in the UFS device. (d) Calculated voltage-dependent transmittances at three different gs and (e) time-dependent transmittance curves in the FFS and UFS devices. Here, the electrode width and gap between patterned electrodes in the FFS device are 3 μm and 4.5 μm, respectively. The transmittance is normalized to two parallel polarizers.

Optics EXPRESS

Both UFS and FFS devices were fabricated using the LC with similar physical properties given above to confirm the switching principle of the UFS device and also much faster decay time in the UFS than that in the FFS device. In the experimental cells, normal FFS electrode structure was tested, in which *g* and width of patterned common electrode was 4.5 μm and 3 μm, respectively and the cell gap was 3 μm because thin cell gap is generally applied for achieving fast response time in the FFS mode. The physical properties of LCs used in the experiment are as follows: $\Delta\varepsilon = 8.0$, $\Delta n = 0.1088$ at 589 nm, rotational viscosity $\gamma = 81$ mPa·s, splay/twist/bend elastic constants = 18.3/8.42/17.7 in pN. Figure 3 shows measured electro-optic characteristics of UFS and FFS devices using LCMS-200 (Sesim Photonics Technology Inc., South Korea).The measured voltage-dependent transmittance curve of the UFS device shows a similar tendency to the calculated result, as shown in Fig. 3(a). We have also observed the POM images in the dark and white states of UFS device, as can be seen in inserted figures in Fig. 3(a). The voltage-off state shows a perfect dark state such that its light leakage level was about half of that of the homogenously aligned FFS device and the white state shows bright stripe lines at both edges of open areas in the voltage-on state. Based on the switching principle of the UFS device, the vertically aligned LC director should tilt down perpendicular to the electrode directions forming two-domain like profile only without any twist. In order to confirm this, the crossed polarizer is rotated by 45° and the result clearly shows a complete dark state, as seen in inset POM image at 10 V. Figure 3(b) shows the measured response times of UFS and FFS devices. The applied voltages for UFS and FFS devices are 10 V and 5.4 V, respectively. The τ_r and τ_d of UFS device is 5.9 ms and 2.4 ms, respectively and especially, the τ_d of the UFS device is more than 4.1 times faster than that of the FFS device. In the given experiments, l_{eff} is 2.3 μm which is slightly smaller than *d* so that the reduction effect on τ_d is decreased compared to the calculated result. Nevertheless, $l_{eff}/d = 0.77$, and $K_3 = 2.1K_2$, so that $\tau_{d\text{-UFS}} \fallingdotseq \tau_{d\text{-IPS}}/4.5$, which explains clearly that the super-fast decay time originates from combined effects of both large magnitude of elastic constants and adoption of non-responsive LC region.

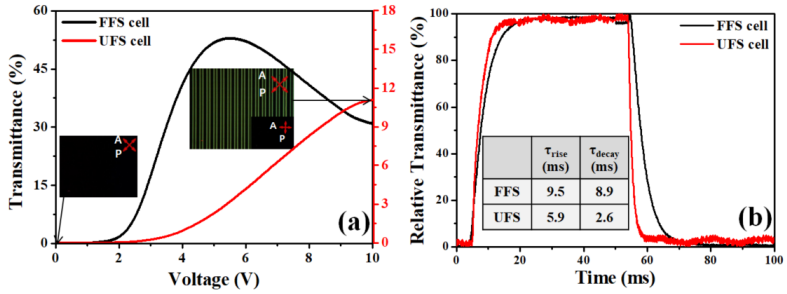

Fig. 3. Measured (a) voltage-dependent and (b) time-dependent transmittance (averaged one over the entire pixel) curves between FFS and UFS devices. The inset POM images represent dark and white states of the UFS device.

Finally, the feasibility of the UFS device for LCDs over 2000 ppi is tested by two- and three-dimensional simulation using TechWiz LCD. Figure 4(a) shows calculated electro-optic characteristics of UFS devices when a pixel pitch is 4 μm and open gap is 2 μm. Here the cell parameters and LC physical properties are the same as abovementioned. The maximal transmittance of two lobes at both edges of the gap is just 18.7% at this pitch, which is quite big drop from 34.2% for the pitch 8 μm with the gap 2 μm, so that the overall transmittance drops to 4.6% from 8.5% (see Fig. 4(c)). In order to improve the transmittance, we tried to optimize several cell parameters such that we have increased cell retardation from 0.4592 μm to 0.6 μm and dielectric anisotropy of LC from 8 to 12.2, and decreased passivation thickness between common and pixel electrodes from 0.3 μm to 0.1 μm. As clearly indicated in Fig. 4(b) and 4(c), we obtained the increased maximal transmittance of two lobes 42.5% and

Optics EXPRESS

overall averaged transmittance 12.4%, whose values are even higher than those in the pitch 8 μm with the gap 2 μm. On the other hand, when the pitch reduces from 8 μm to 4 μm, the response time becomes more than twice times faster in the short pitch, owing to reduced both l and $l_{\text{eff.}}$ as indicated in Fig. 4(d).

Applying those optimized parameters, three-dimensional calculation defining 2000 ppi is performed. Figure 5 shows top view image of the transmittance profile and the transmittance along horizontal electrode position when a pixel pitch is 4 μm, open gap is 2 μm, and distance between pixel electrodes is 1 μm. The transmittance was evaluated when three pixels in second row of the 3 x 3 pixels are on state, as shown in Fig. 5(a). The transmittance in four sides of a rectangular open gap occurs due to oblique electric field. The transmittance at center area of the open gap is not occurred because LC directors are tightly hold by a vertical electric field generated by common electrode on top substrate and pixel electrode on bottom substrate forming an imaginal wall. The light leakage does not occur between neighboring pixels in horizontal direction because the LC directors retain its original state of vertical alignment by the force of a symmetrical electric field generated in both directions, as shown in Fig. 5(b). However, some level of transmittance penetrates over neighboring pixels in vertical direction due to overall improved transmittance in the optimized condition, however, it can be blocked mostly because opaque gate lines exist below these regions. Consequently, with the electrode geometry given, a suppression of the inter-pixel interference on all sides of one pixel is possible, indicating that the high resolution over 2000 ppi in about 3" UFS-LCD can be achieved.

Overall, we show the UFS device is suitable to ultra-high resolution TFT-LCD with fast response time and high contrast; however, still relatively low transmittance and high operating voltage are drawbacks, which needs to be improved. The improvement and optimization of overall electro-optic performance is under progress.

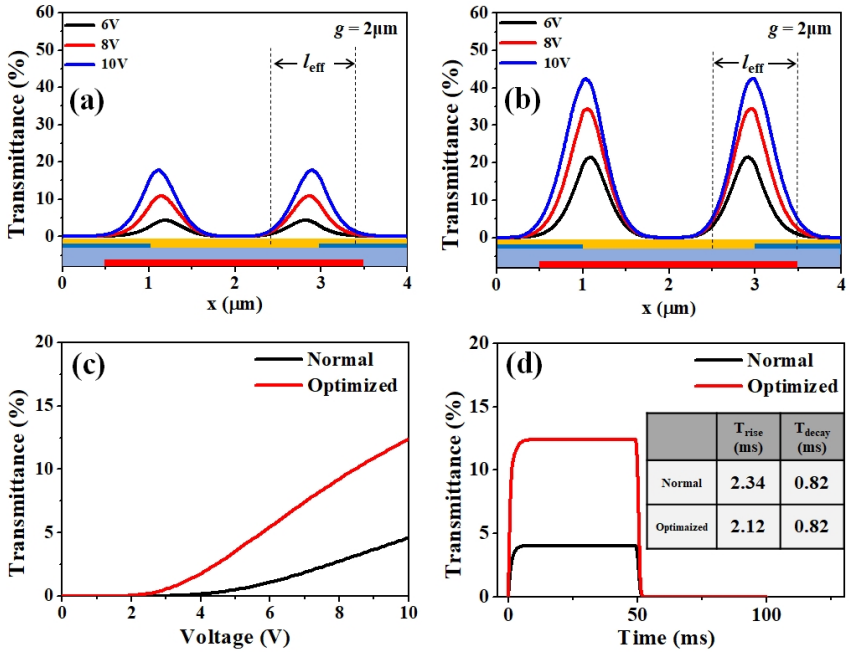

Fig. 4. Calculated electrode-position dependent transmittances at three different voltages when the pixel pitch is 4 μm with gap of 2 μm in the normal (a) and the optimized (b) UFS device. (c) Calculated voltage-dependent transmittances and (d) Time-dependent transmittance curves at two different device conditions. Here, the transmittance is normalized to two parallel polarizers. When the pixel pitch reduces from 8 μm to 4 μm, both l and $l_{\text{eff.}}$ become reduced, resulting in much faster response times in the reduced pitch.

Optics EXPRESS

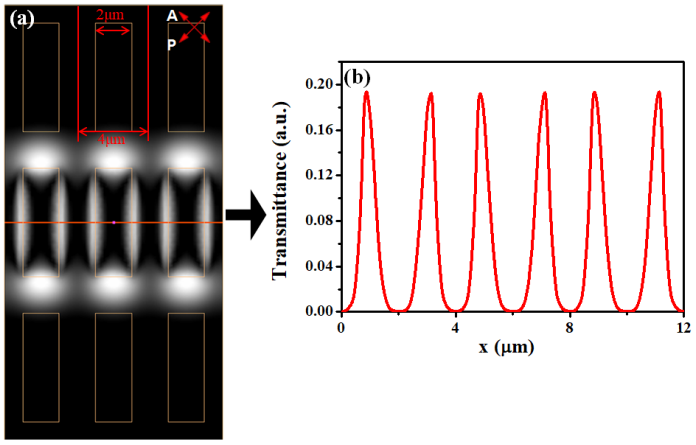

Fig. 5. Evaluation of optical crosstalk considering 3 x 3 pixels using three-dimensional simulator: (a) Top-view of transmittance profile when three pixels in second row are on state, and (b) Transmittance profile along horizontal direction in which it is defined well within 4 μm.

4. Conclusion

We have proposed an ultra-fast switching vertically aligned liquid crystal display (LCD) with use of a LC with positive dielectric anisotropy, which demonstrates superior electro-optic performance such as high resolution, super-fast response time, and high contrast ratio for virtual reality-head mounted displays. This device has no optical cross talk in inter-pixel even if the pixel pitch is 4 μm because non-responsive LC region is well kept by both vertical and non-existence of an electric field, which makes it realize high resolution over 2000 ppi. Also, the device shows an excellent dark state because liquid crystals are initially vertically aligned like conventional vertical alignment device. Especially, the decaying time of the proposed device can be just few ms because its elastic restoring force is associated with both bend elastic constant and also formation of non-response LC zone with a short pitch. Consequently, we demonstrated a suitable design for realization of VR-HMDs that require high refresh rate and high definition.

Funding

Basic Science Research Program through the National Research Foundation of Korea (NRF) funded by Ministry of Education (2016R1D1A1B01007189).

References

1. N. Ueda, K. Okada, S. Uchida, K. Yamamoto, and H. Yoshida, “Liquid crystal display with ultra highresolution and super fast response giving super reality to VR application,”Proc. of the 23rdInternational Display Workshops in conjunction with Asia display (Society for Information Display, Fukuoka, Japan), 281–284 (2016).
2. S. H. Lee, S. L. Lee, and H. Y. Kim, “Electro-optic characteristics and switching principle of a nematic liquid crystal cell controlled by fringe-field switching,” Appl. Phys. Lett. **73**(20), 2881–2883 (1998).
3. M. S. Kim, P. J. Bos, D.-W. Kim, D.-K. Yang, J. H. Lee, and S. H. Lee, “Flexoelectric effect in an in-plane switching (IPS) liquid crystal cell for low-power consumption display devices,” Sci. Rep. **6**(1), 35254 (2016).
4. M. S. Kim, P. J. Bos, D.-W. Kim, C.-M. Keum, D.-K. Yang, H. G. Ham, K.-U. Jeong, J. H. Lee, and S. H. Lee, “Field-symmetrization to solve luminance deviation between frames in a low-frequency-driven fringe-field switching liquid crystal cell,” Opt. Express **24**(26), 29568–29576 (2016).
5. M. Kim, H. G. Ham, H.-S. Choi, P. J. Bos, D.-K. Yang, J. H. Lee, and S. H. Lee, “Flexoelectric in-plane switching (IPS) mode with ultra-high-transmittance, low-voltage, low-frequency, and a flicker-free image,” Opt. Express **25**(6), 5962–5971 (2017).
6. M. S. Kim, H. S. Jin, S. J. Lee, Y.-H. Shin, H. G. Ham, D.-K. Yang, P. J. Bos, J. H. Lee, and S. H. Lee, “Liquid crystals for superior electro-optic performance display device with power-saving mode,” Adv. Opt. Mater. **6**(11), 1800022 (2018).

Optics EXPRESS

7. T. Mastushima, K. Okazaki, Y. Yang, and K. Takizawa, "New fast response time in-plane switching liquid crystal mode," SID Symposium Digest of Technical Papers **46**, 648–651 (2015).
8. T. Mastushima and K. Takizawa, "Analysis of novel IPS mode for tast response," Proc. of the 22nd International Display Workshops (Society for Information Display, Otsu, Japan), 44–47 (2015).
9. T.-H. Choi, S.-W. Oh, Y.-J. Park, Y. Choi, and T.-H. Yoon, "Fast fringe-field switching of a liquid crystal cell by two-dimensional confinement with virtual walls," Sci. Rep. **6**(1), 27936 (2016).
10. T. Katayama, S. Higashida, A. Kanashima, K. Hanaoka, H. Yoshida, and S. Shimada, "Development of in-plane super fast response (ip-SFR) LCD for VR-HMD,"SID Symposium Digest of Technical Papers **49**, 671–673 (2018).
11. T. Matsushima, K. Seki, S. Kimura, Y. Iwakabe, T. Yata, Y. Watanabe, S. Komura, M. Uchida, and T. Nakanura, "Optimal fast-response LCD for high-definition virtual reality head mounted display," SID Symposium Digest of Technical Papers **49**, 667–670 (2018).
12. K. Ono and I. Hiyama, "The latest IPS pixel structure suitable for high resolution LCDs," Proc. of the 19th International Display Workshops in conjunction with Asia Display (Society for Information Display, Kyoto, Japan), 933–936 (2012).
13. K. Ono and H. Matsukawa, "High performance IPS technology suitable for high resolution LCDs," Proc. of the 20th International Display Workshops (Society for Information Display, Sapporo, Japan), 24–25 (2013).
14. R. A. Soref, "Field effects in nematic liquid crystals obtained with interdigital electrodes," J. Appl. Phys. **45**(12), 5466–5468 (1974).
15. S. H. Lee, H. Y. Kim, I. C. Park, B. G. Rho, J. S. Park, H. S. Park, and C. H. Lee, "Rubbing-free, vertically aligned nematic liquid crystal display controlled by in-plane field," Appl. Phys. Lett. **71**(19), 2851–2853 (1997).
16. F. Gou, H. Chen, M.-C. Li, S.-L. Lee, and S.-T. Wu, "Submillisecond-response liquid crystal for high-resolution virtual reality displays," Opt. Express **25**(7), 7984–7997 (2017).
17. H. Chen, F. Peng, F. Gou, Y.-H. Lee, M. Wand, and S.-T. Wu, "Nematic LCD with motion picture response time comparable to organic LEDs," Optica **3**(9), 1033–1034 (2016).